Available online at www.sciencedirect.com
ScienceDirect
Trans. Nonferrous Met. Soc. China 22(2012) 740−746
Transactions of Nonferrous Metals Society of China
www.tnmsc.cn

# Safe mining technology of undersea metal mine

PENG Kang[1,2], LI Xi-bing[1,2], WAN Chuan-chuan[1,2], PENG Shu-quan[1,2], ZHAO Guo-yan[1,2]

1. School of Resources and Safety Engineering, Central South University, Changsha 410083, China;
2. Hunan Key Laboratory of Resources Exploitation and Hazard Control for Deep Metal Mines Central South University, Changsha 410083, China

Received 10 March 2011; accepted 9 September 2011

**Abstract:** Xinli district of Sanshandao Gold Mine is the first subsea metal mine in China. To achieve 6 kt/d production capacity under the premise of safe mining, high-intensity mining might destroy the in-situ stress filed and the stability of rockmass. According to sampling and testing of ore-rock and backfill and in-situ stress field measurement, safety factor method calculation model based on stress—strain strength reduction at arbitrary points and Mohr-Coulomb yield criterion was established and limit displacement subsidence values under the safety factor of different limit stoping steps were calculated. The results from three years in-situ mining and strata movement monitoring using multi-point displacements meter showed that the lower settlement frame stope hierarchical level filling mining method, mining sequence are reasonable and rockmass stability evaluation using safety factor method, in-situ real-time monitoring can provide the technical foundation for the safety of seabed mining.

**Key words:** subsea bedrock mining; frame stope upward horizontal slicing and filling mining method; safety factor method; multi-point displacement measurement

## 1 Introduction

With the increasing exhausted shallow mineral resources, mining coastal deposits is imperative at home and abroad. Dikes embedded in seaside bedrock or layered solid deposits are called undersea metal mine [1]. Because the physico-mechanical properties of ore and surrounding rock and the morphologies of ore body are similar to those of land deposits, mining methods of land deposits can be referred. At present, there are experiences from mining undersea metal mines successfully in England, Finland, Australia and China, whose development methods are divided into vertical shaft exploication in the artificial island, vertical shaft exploication on the coast and precast tunnel-closed shaft exploication based on the distance between ore body and coastline. In Japan, a coal mine was poured into by plenty of seawater due to fractures and offsets appearing in the aquifuge in the process of subsea mining, which caused severe consequences [2]. Xinli district of Sanshandao Gold Mine is the first subsea metal mine in China, whose ore body is located under the sea at the range of tens to hundreds of meters. Several meters thick permanent ore pillar between ore body and seawater is used as the aquifuge, and in-situ stress field is destroyed easily if mining improperly, and then it will bring potential safety hazards in the mining process.

Finite Element Method (FEM) strength reduction method has the advantages of both numerical analysis method and classical limit analysis method. ZIENKIEWICA and HUMPHESON [3] have suggested it to analyze slope ability as early as 1975. UGAI and LESHCHINSKY [4] have introduced it to elasto-plastic FEM to analyze slope stability in three dimensions. DUNCAN [5] has pointed out that slope safety factor can be defined as reduction degree of soil shear strength when slope happens to be in the state of critical failure. Recently, FEM strength reduction method to analyze slope stability has been accepted globally and has been used in designing supporting methods practically in our country. In the present work, safety factor method based on stress—strain strength reduction at arbitrary points in the FEM strength reduction method and Mohr-Coulomb

**Foundation item:** Project (10872218) supported by the National Natural Science Foundation of China; Project (2010CB732004) supported by the National Key Basic Research Program of China; Project (20090461022) supported by the National Postdoctoral Foundation of China; Project (11MX21) supported by the Students' Innovation Project Aubsidize Award of Arcelor Mittal
**Corresponding author:** PENG Kang; Tel: +86-15974269965; E-mail: pengkang86121@126.com
DOI: 10.1016/S1003-6326(11)61239-9

yield criterion is introduced to analyze the stability of rockmass of stopes after backfilling. Meanwhile, a monitoring system with multi-point displacement meters is used. The coastline length is about $3.2\times10^4$ km and there are 6500 or more islands in our country. Research on safety mining technology of undersea mineral deposits is significant under the period of lacking resource.

## 2 Project profile

### 2.1 Geology and development

The ore body is composed of beresitization fractured rock and beresitization granitic fractured rock. The mineralization is continuous. The average strike length is 900 m and average true thickness is 25 m. The strike angle is from 42° to 80° and the dip is from 33° to 67°. The hanging wall rocks are sericitization fractured rock and sericitization granitic fractured rock; the foot wall rocks are beresitization fractured rock and beresitization granitic fractured rock. The development form is as follows: it is mined by advancing main shaft to hoist ore, special air shaft using freezing method and auxiliary shaft to hoist miners, and equipment raise (also used as filling raise) to hoist barren rock using curtain grouting method. Each roadway gets to foot wall through the cross drift, where main haulage drift at every level is advancing (see Fig. 1).

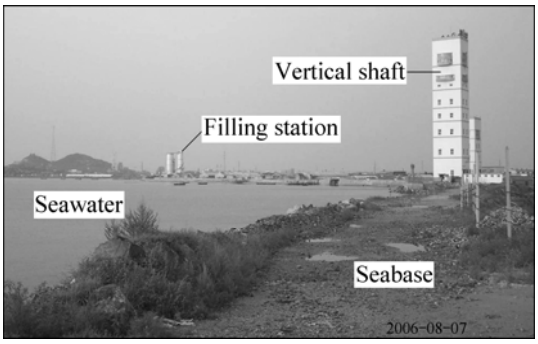


**Fig. 1** Mining sketch of Sanshandao Gold Mine, China

### 2.2 Hydrogeology

At present, the mining level in Sanshandao Gold Mine is beneath −165 m, with a beforehand 130 m-thick isolated layer, at the top of which is the water volume with a height of 13 m. According to synthesized analysis to hydrological conditions in the mining region, the specific capacity is less than 0.001 L/(s·m), which indicates the rockmass is waterless and the bottom aquifuge of Quaternary system, and the combination part of Quaternary system and bedrock spreads continuously in the whole mining region with the thickness of 0.8−10.0 m. The drilling data show that the rock consists of sandy clay and silty clay, belonging to the leftover slope wash formed by weathering, and the core is columnar. It is indicated that microscopic particles are schistose and they mostly come into contact with edge−surface and surface–surface by sampling at 22# well to the east of main shaft and its magnifying image by 5000 times (see Fig. 2). Besides, the microstructure is porous with flocculent structure, and the pore is cluster, presenting in the form of long strips. The diameter of the pore is about 1 μm with a poor connectivity. So, it has a low permeability and can be used as the aquifuge when mining under no disturbances.

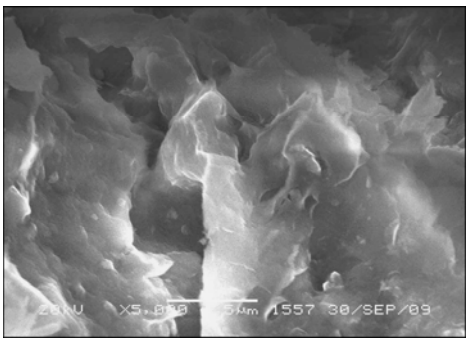


**Fig. 2** SEM image of yellow silty clay

According to the criteria [6], the basic mechanical property tests to clay were carried out. The results show that the density of the clay, water content, internal friction angle (under saturation and no drainage), cohesion and permeability are 1.770 g/cm$^3$, 25.03%, 3.58°, 4.89 kPa and $5.13\times10^{-8}$ cm/s, respectively. The aquifuge of Quaternary system obstructs the recharge of underground water from water zone in the foot wall. The influence of seepage has not been taken into account when calculating by simplifying the hydrological conditions of ore deposits.

### 2.3 Rock mechanics parameters

Based on in-situ investigations, sampling and laboratory experiment, physico-mechanical parameters of ore and rock are shown in Table 1.

**Table 1** Physico-mechanical parameters of ore and rock

| Type | Compressive strength/MPa | Internal friction angle/(°) | Cohesion/MPa | Density/(g·cm$^{-3}$) | Poisson ratio | Elastic module/GPa | Tensile strength/MPa |
|---|---|---|---|---|---|---|---|
| Foot wall | 28.83 | 35.0 | 0.88 | 2.64 | 0.24 | 5.30 | 1.06 |
| Ore body | 22.64 | 32.0 | 0.50 | 2.71 | 0.19 | 3.48 | 0.60 |
| Hanging wall | 21.38 | 32.2 | 0.26 | 2.68 | 0.20 | 4.03 | 0.30 |

### 2.4 In-situ stress field measurement

In-situ stress field is composed of gravitational stress field and tectonic stress field [7]. The in-situ stress field in Sanshandao Gold Mine, China, was measured with UPM40 made in Sweden. The measuring points were selected away from areas of stress concentration, faults, fractured rock zones, fault developed zones, large gob areas and chambers. Three measuring points were set at −240 m level, two measuring points were set at −400 m level, and one measuring point was set at −165 m level. All six measuring points were set in rockmass and ore body newly excavated. Based on principle stress calculation results of each measure point, equatorial horizon projection map was drafted on Wu's net (Fig. 3) in the ascending order of burial depth. In Fig. 3, $\sigma_1$ is the first principle stress, $\sigma_2$ is the second principal stress and $\sigma_3$ is the third principle stress.

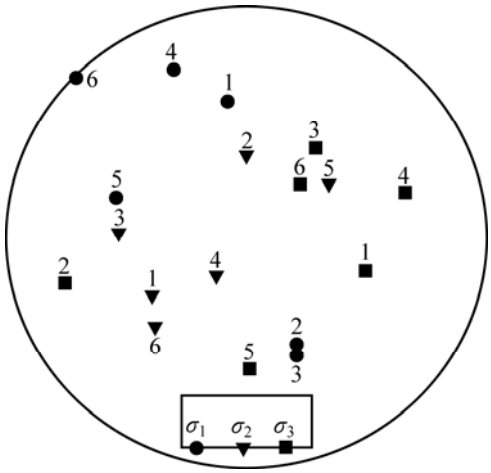


**Fig. 3** Equatorial horizon projection of principal stress direction of six measuring points

The maximum horizontal principle stress, the minimum horizontal principle stress and vertical principle stress of those six measuring points were regressed linearly using least square method. The law of the maximum principle stress $\sigma_{hmax}$, the minimum principle stress $\sigma_{hmin}$ and vertical principle stress $\sigma_z$ versus buried depth are given as:

$$\sigma_{hmax} = 0.11 + 0.0539z \quad (1)$$

$$\sigma_{hmin} = 0.13 + 0.0181z \quad (2)$$

$$\sigma_z = 0.08 + 0.0315z \quad (3)$$

where $z$ is the depth in the vertical direction (m). The unit of principle stress is MPa.

The measurement results show that the strike of the maximum principle stress is North-West. Regional stress field and main controlling fault altered belt whose strike is North-East are featured with compression−shear, which prevents hydraulic conductivity. This is the critical reason why water inflow is small in the main controlling fault altered belt of Sanshandao Gold Mine, China.

## 3 FEM numerical analysis

### 3.1 Basic principle

Safety factor method [8−10] based on stress—strain strength reduction process at arbitrary points in the FEM strength reduction theory and Mohr−Coulomb yield criterion is introduced into the present work, which evaluates the stability of rockmass in the dynamic undersea mining process [11]. Basic principle is shown in Fig. 4.

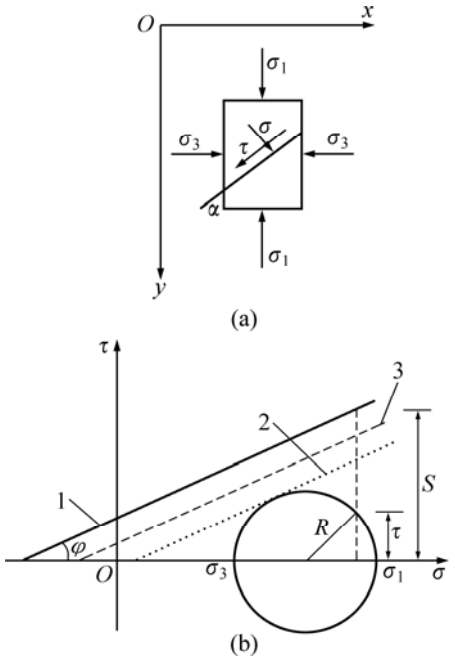


**Fig. 4** Strength reduction process of stress—strain at arbitrary points: (a) Stress distribution at one point; (b) Mohr-coulomb strength reduction process; 1—Mohr-coulomb strength line; 2—Mohr−coulomb post-reduction strength line in the limit state; 3—Mohr−coulomb strength line in the reduction process

where $\sigma_1$ is the first principal stress; $\sigma_3$ is the third principal stress; $\sigma$ is the normal stress; $\tau$ is the shear stress; $\alpha$ is the angle between the potential glide plane and the first principal stress; $R$ is the radius of Mohr stress circle; $\varphi$ is the dip of Mohr-coulomb strength line.

Rock shear strength is relative to stress field in rockmass. When shear stress on the failure plane surpasses shear strength, shear failure will occur. Then static equilibrium conditions should be satisfied as follows:

$$\sum F_x = 0 : \sigma A\cos\alpha - \tau A\sin\alpha = \sigma_3 A\cos\alpha \quad (4)$$

$$\sum F_y = 0 : \sigma A\sin\alpha + \tau A\cos\alpha = \sigma_1 A\sin\alpha \quad (5)$$

where $\alpha$ is the angle between potential glide plane and the first principle stress; $A$ is the glide plane area.

According to transformation relation among stress components at an arbitrary inclined plane, normal and tangential stresses on the failure plane are attained respectively by simultaneous solving Eqs. (4) and (5):

$$\sigma = \sigma_1 \sin^2 \alpha + \sigma_3 \cos^2 \alpha = (\sigma_1 - \sigma_3)\sin^2 \alpha + \sigma_3 \quad (6)$$

$$\tau = (\sigma_1 - \sigma_3)\sin \alpha \cos \alpha \quad (7)$$

According to Mohr−Coulomb yield criterion, shear strength $\sigma_c$ on the plane is expressed as

$$\sigma_c = \sigma \tan \varphi + c = \left( \frac{\sigma_1 + \sigma_3}{2} + \frac{\sigma_1 - \sigma_3}{2} \cos \right) \tan \varphi + c \quad (8)$$

where $\varphi$ and $c$ are internal friction angle and cohesion on the potential glide plane, respectively.

The shear safety factor ($K$), is defined as the ratio of shear strength to actual shear stress:

$$K = \frac{\sigma_c}{\tau} \quad (9)$$

After substituting Eqs. (6) and (7) into Eq. (9), shear safety factor is related to the angle $\alpha$ of the plane. It is indicated that different planes through a point have different shear safety factors. Therefore, the minimum shear safety factor is the potential failure plane, and $\alpha$ can be obtained by calculating the minimum value $dK/d\alpha=0$,

$$\alpha = \arccos \left( - \frac{\frac{\sigma_1 - \sigma_3}{2}}{\frac{\sigma_1 + \sigma_3}{2} + c \cot \varphi} \right) \quad (10)$$

The safety factor ($K$) in the FEM strength reduction method is an index that can be used to evaluate the stability of elements under complex stress state, also can evaluate the level of plastic yielding, and can directly reflect rockmass stability under stress conditions. It has direct relation with rockmass strength, stress and strength criteria. When $K$>1, elements remain undamaged (inside the yield surface); when $K$<1, elements have been damaged (outside the yield surface); when $K$=1, it is the critical state (on the yield surface).

### 3.2 Finite element model in dynamic stoping

According to the present mining conditions, ore body at −165 m level is completely mined by frame stope mechanical upward horizontal slicing and filling method (see Fig. 5) and roofs are contacted by backfilling. Ore body at −240 m level is being mined.

The length of ore body at −240 m level is about 900 m and nine panels are divided along the strike of ore body (see Fig. 6). Each panel is 100 m long along the strike and 40 m high. The sill pillar is 5 m high and the crown pillar is 2 m high. The span of point pillars is 16 m along the strike and 12 m perpendicular to the strike. The rib pillar is 4 m wide between the panels. According to the requirement of 6000 t/d production capacity, three panels are mined simultaneously each time. Based on the stoping plan——"two stope panels" used in development engineering: the ninth, sixth and third panels are mined firstly→the eighth and fifth panels are mined secondly→the seventh, fourth and first panels are mined thirdly.

### 3.3 Calculation results of safety factor after stoping in each panel

The stability of rockmass during the process of limit stoping in each panel is analyzed based on the calculation results of numerical model with mechanical

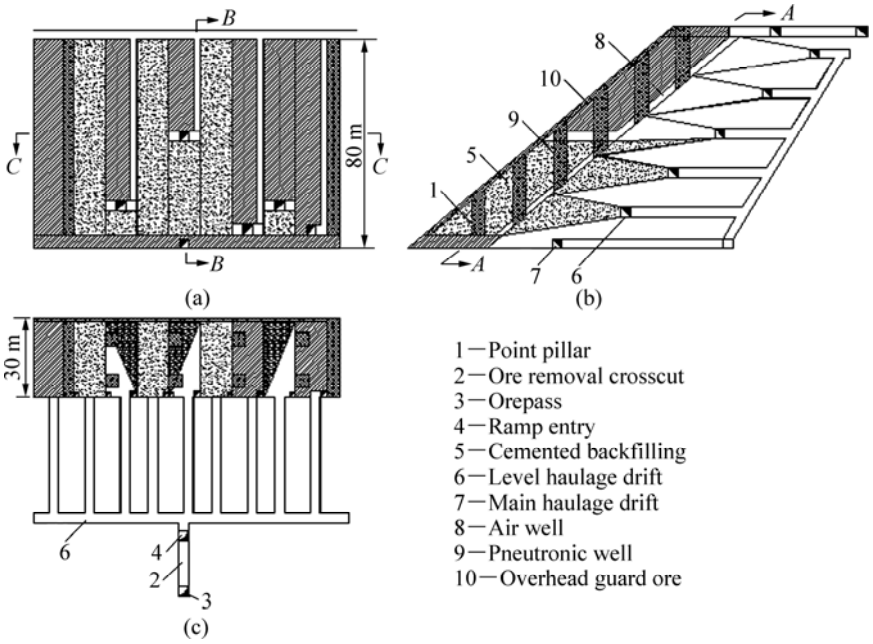


**Fig. 5** Hierarchical level filling mining method for lower settlement frame stope: (a) $A$−$A$ section; (b) $B$−$B$ section; (c) $C$−$C$ section

parameters and in-situ stress. The equivalent nephogram described by safety factor of the first principle stress and the third principle stress in finite elements after stoping is shown in Fig. 7. Because of the bad stability of stope roof, roof falling in large areas is possible if stope roof and rib pillar are destroyed. When checked by safety factor, its value around the stope roof should be more than 1 and get close to 1.5; the whole stope is in the safe and stable state if safety factor of every point in the rockmass around the roof is more than 1.5 [12−16].

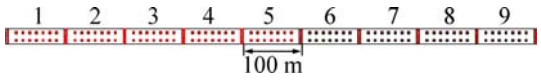


**Fig. 6** Divided finite element model of panel

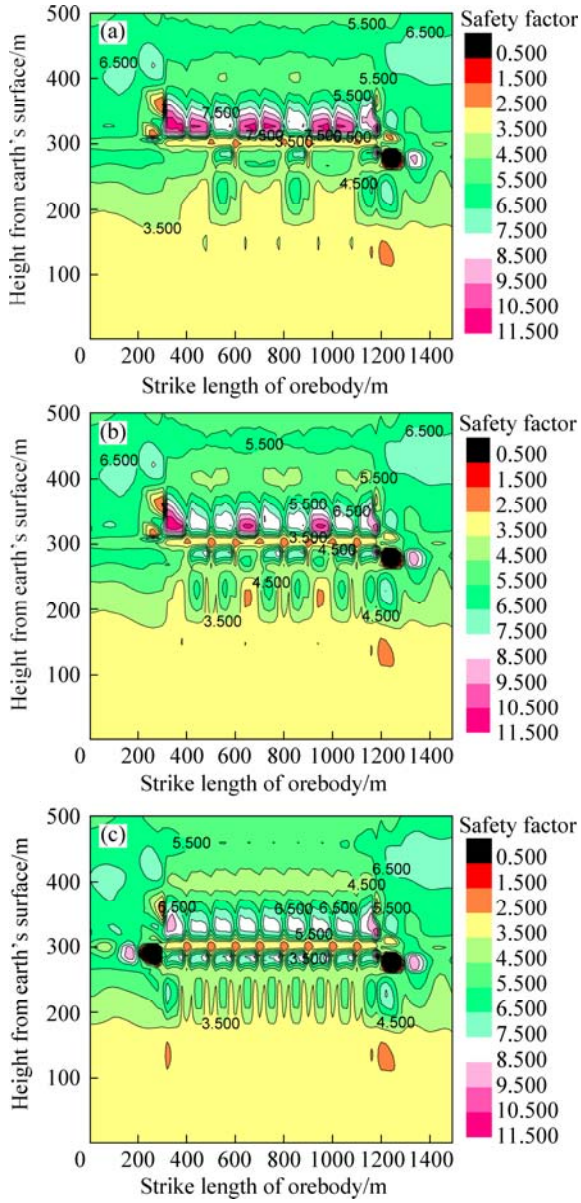


**Fig. 7** Equivalent nephogram of safety factor of step mining: (a) The first step mining; (b) The second step mining; (c) The third step mining

Figure 7 shows that instability zone in the stope is concentrated in roof at −240 m level and floor at −200 m level (height range: −202 m to −195 m), and safety factor changes between 2.5 and 3.5.

### 3.4 Subsidence curves after stoping in different panels

Limit displacement subsidence curves are shown in Fig. 8 under the safety factor of different limit stoping steps.

The maximum subsidence value is 0.004 m after the first stoping step and 0.008 m after the second stoping step and 0.012 m after the third stoping step. The subsidence increment is uniform under different stoping steps and it will not result in mine inundation accident due to uneven subsidence of Quaternary system aquifuge.

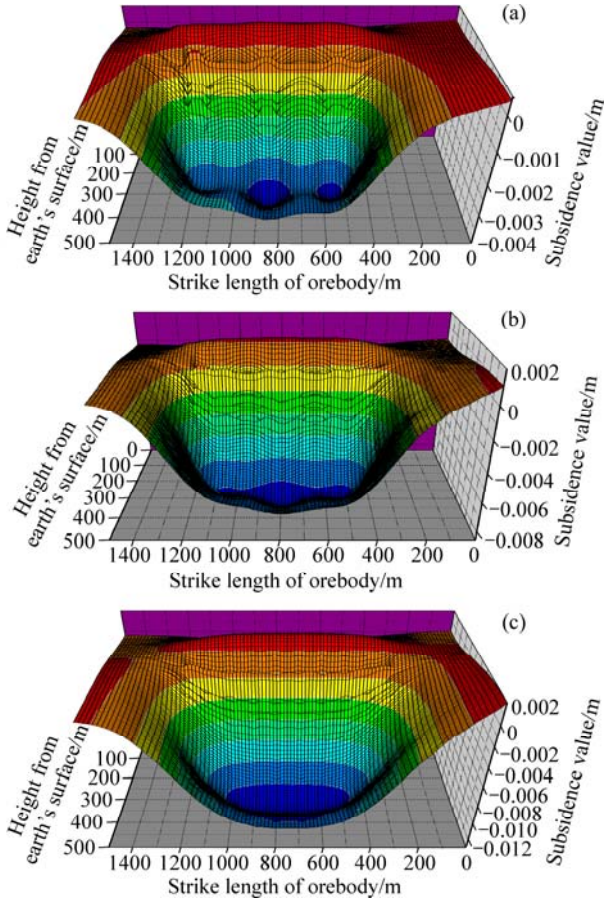


**Fig. 8** Ore−rock's subsidence curve during mining (unit: m): (a) The first step mining; (b) The second step mining; (c) The third step mining

## 4 Monitoring and analysis of strata movement

### 4.1 Performance of multi-point displacement meter

The multi-point displacement meter used in Sanshandao Gold Mine, China, consists of several intelligent displacement meters, transmission rods,

anchor heads and so on. Within the scope of 1 $m^2$, many holes were drilled. The multi-point displacement meter is composed of several ones for single point [17]. The displacement meter should be fixed in the upward holes whose design height were respectively 10 m, 20 m, 30 m in underground chamber. The hole diameter was 40 mm. The upward holes drilled by engineering geological drilling rig and structure chart of multi-point displacement monitoring system in Xinli district are shown in Fig. 9, from which vertical deformation subsidence law of strata on different heights can be observed.

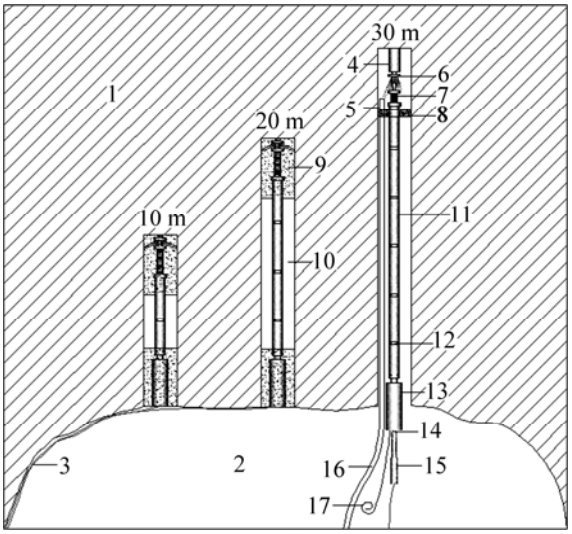


**Fig. 9** Sketch map of multi-point displacement meter measurement configuration: 1—Rockmass; 2—Chamber; 3—Hydraulic cable; 4—Cement roll; 5—Grouting pipe; 6—Anchor head; 7—Bolt; 8—Sponge; 9—Slurry; 10—Drill hole; 11—Displacement transmission rod; 12—Pipe joint; 13—PVC protective tube; 14—Measuring bar; 15—Displacement meter; 16—Grouting pipe; 17—Thin iron wire

### 4.2 Monitoring result analysis

According to numerical simulation results, the worst safety factor of rib pillar and relative stope roof and floor is 2.5−3.5 in three panels at −240 m level after their limit stoping and backfill. The results are proved to be correct. The maximum subsidence value of ground is 4 mm. Site monitoring results of strata movement show that values of multi-point displacement meter increase with ore mining. The maximum deformation within 215 d is 2.2 mm, and most data are below 1.8 mm, which indicates that deformation is little and mining is safe. On one hand, there were regular point pillars of 4 m×4 m in stopes, whose span was 16 m along the strike, 12 m perpendicular to the strike. The sill pillar was 5 m, and the crown pillar was 2 m. On the other hand, tailing backfill was done after each slice stoping. The last slice adopted roof-contacted backfilling after level ore was mined out. The exposure time of gob area was short. Backfilling body had sufficient strength and roof-contacted effect was good. Ground pressure was under good control, which was crucial to the stability of rockmass and ensured safe mining under the sea.

## 5 Conclusions

According to sampling and testing of ore-rock and backfill and in-situ stress field measurement, safety factor method calculation model based on stress—strain strength reduction at arbitrary points and Mohr−Coulomb yield criterion is established and limit displacement subsidence values under the safety factor of different limit stoping steps are calculated. The results from three years in-situ mining and strata movement monitoring using multi-point displacement meter show that the lower settlement frame stope hierarchical level filling mining method, mining sequence and rockmass stability evaluation using safety factor method are reasonable. The safety factor method of stability evaluation and in-situ strata measurement can provide technical guidance for engineering. Strata displacement should be monitored for long time and the data should be dealt with and analyzed. By observing the variation of those data, deformation tendency of strata movement was gained, which can be used as a forecasting means for hazards and provide technical support for the safety of seabed mining in Sanshandao Gold Mine.

## References

[1] PENG Kang, LI Xi-bing. Optimization of frame stope structure parameters based on response surface method in under-sea mining [J]. Journal of Central South University: Science and Technology, 2011, 42(8): 2417−2431. (in Chinese)

[2] ZHAO Guo-yan. Study on the safety mining technology of seabed hard rock [J]. China Safety Science Journal, 2009, 19(5): 159−166. (in Chinese)

[3] ZIENKIEWICA O C, HUMPHESON C, LEVIS R W. Associated and non-associated visco-plasticity and plasticity in soil mechanics [J]. Geotechnique, 1975, 25(4): 671−689.

[4] UGAI K, LESHCHINSKY D. Three-dimensional limit equilibrium and finite element analyses: A comparison of results [J]. Soils and Foundations, 1995, 35(4): 1−7.

[5] DUNCAN J M. State of the art: Limit equilibrium and finite-element analysis of slopes [J]. Journal of Geotechnical Engineering, 1996, 122(7): 577−596.

[6] GB/T50123—1999 Standard of soil test method [S]. Beijing: China Planning Press, 1999.

[7] MA Chun-de, XU Ji-cheng, CHEN Feng. Research on in-situ stress measurement and its distribution law in Dahongshan iron mine [J]. Metal Mine, 2007(8): 42−45. (in Chinese)

[8] ZHENG Hong, LI Chun-guang, LEE Zhao-fen, GE Xia-run. Finite element method for solving the factor of safety [J]. Chinese Journal of Geotechnical Engineering, 2002, 24(5): 323−328. (in Chinese)

[9] SHU Gu-sheng, PENG Wen-xiang, HE Zhong-ming, ZHONG Zheng-qiang. Element safety factor in rock stability estimation and its influence factors [J]. Science & Technology Review, 2009, 27(16):

66−68.
[10] LI Shu-chen, LI Shu-cai, XU Bang-shu. Minimum safety factor method for stability analysis of surrounding rockmass of tunnel [J]. Rock and Soil Mechanics, 2007, 28(3): 549−554.
[11] PENG Kang, LI Xi-bing. Dynamic simulation of reasonable stoping sequence in middle section of panel in sanshandao gold mine [J]. Mining and Metallurgical Engineering, 2010, 30(3): 8−12. (in Chinese)
[12] GAO En-zhi, LI Hong-wei, KOU Hong-chao, CHANG Hui, LI Jin-shan, ZHOU Lian. Influences of material parameters on deep drawing of thin-walled hemispheric surface part [J]. Transactions of Nonferrous Metals Society of China, 2009, 19(2): 433−437.
[13] Microstructure of spray formed Al-Zn-Mg-Cu alloy with Mn addition [J]. Transaction Nonferrous Metals Society of China, 2011, 21(1): 9−14.
[14] Detoxification of chromium-containing slag by Achromo- bacter sp. CH-1 and selective recovery of chromium [J]. Transaction Nonferrous Metals Society of China, 2010, 20(8): 1500−1504.
[15] JIANG Yao-dong, LIU Wen-gang, ZHAO Yi-xin, et al. Study on surrounding rock stability of deep mining in Kailuan mining group [J]. Chinese Journal of Rock Mechanics and Engineering, 2005, 24(11): 1857−1862. (in Chinese)
[16] ZHENG Ying-ren, QIU Chen-yu, ZHANG Hong, WANG Qian-yuan. Exploration of stability analysis methods for surrounding rocks of soil tunnel [J]. Chinese Journal of Rock Mechanics and Engineering, 2008, 27(10): 1968−1980. (in Chinese)
[17] WANG Jing-chun, HOU Wei-hong, MO Xun-tao. Preliminary research on safety evaluation for subsea tunnel construction [J]. Chinese Journal of Rock Mechanics and Engineering, 2007, 26(S2): 3756−3762. (in Chinese)
[18] ZHANG Li-ming, ZHENG Ying-ren, WANG Zai-quan, WANG Jian-xin. Application of strength reduction finite element method to road tunnels [J]. Rock and Soil Mechanics, 2007, 28(1): 97−106.
[19] LI Xi-bing, LIU Zhi-xiang, PENG Kang, ZHAO Guo-yan, PENG Shu-quan. Theory and practice of rock mechanics related to exploitation of undersea metal mine [J]. Chinese Journal of Rock Mechanics and Engineering, 2010, 29(10): 1945−1953. (in Chinese)
[20] YOU Chu-nan, BAI Yun. A new method of multi-point displacement measurement in surrounding rocks of under ground engineerings [J]. Rock and Soil Mechanics, 2000, 21(2): 138−140.

# 金属矿滨海基岩的安全开采技术

彭 康[1,2]，李夕兵[1,2]，万串串[1,2]，彭述权[1,2]，赵国彦[1,2]

1. 中南大学 资源与安全工程学院，长沙 410083；
2. 中南大学 深部金属矿产开发与灾害控制湖南省重点实验室，长沙 410083

**摘 要**：三山岛金矿新立矿区是我国第一个滨海开采的金属矿山，要使生产能力在安全开采的前提下达到 6 kt/d，高强度开采势必扰动原岩地应力场，破坏矿岩的稳定性。通过矿岩、充填尾砂取样、试验及原岩地应力场的测定，建立任意点的应力—应变强度折减过程与莫尔−库仑准则条件下的安全系数法计算模型，计算出矿山在动态回采过程中矿岩的安全系数及其相对应的极限位移沉降量。通过为期 3 年的现场滨海开采实践及多点位移计岩移监测，结果表明：低沉降框架式上向分层充填法、采场结构参数、盘区回采顺序及安全系数法矿岩稳定性分析、现场实时监测为滨海基岩开采提供了技术支撑。

**关键词**：滨海基岩开采；框架式上向水平分层充填法；安全系数法；多点位移监测

**(Edited by YANG Hua)**